Leakage mechanisms of self-assembled (BiFeO3)0.5:(Sm2O3)0.5 nanocomposite films

H. Yang, H. Wang, G. F. Zou, M. Jain, N. A. Suvorova et al.

Citation: Appl. Phys. Lett. **93**, 142904 (2008); doi: 10.1063/1.3000013
View online: http://dx.doi.org/10.1063/1.3000013
View Table of Contents: http://apl.aip.org/resource/1/APPLAB/v93/i14
Published by the American Institute of Physics.

Leakage mechanisms of self-assembled $(BiFeO_3)_{0.5}:(Sm_2O_3)_{0.5}$ nanocomposite films

H. Yang,[1,a)] H. Wang,[2] G. F. Zou,[1] M. Jain,[1] N. A. Suvorova,[1] D. M. Feldmann,[1] P. C. Dowden,[1] R. F. DePaula,[1] J. L. MacManus-Driscoll,[3] A. J. Taylor,[1] and Q. X. Jia[1,a)]
[1]*Materials Physics and Applications Division, Los Alamos National Laboratory, Los Alamos, New Mexico 87545, USA*
[2]*Department of Electrical and Computer Engineering, Texas A&M University, College Station, Texas 77843-3128, USA*
[3]*Department of Materials Science and Metallurgy, University of Cambridge, Cambridge CB2 3QZ, United Kingdom*

(Received 17 April 2008; accepted 20 September 2008; published online 10 October 2008)

Nanocomposite $(BiFeO_3)_{0.5}:(Sm_2O_3)_{0.5}$ films were deposited on (001) oriented Nb-doped $SrTiO_3$ substrates by pulsed laser deposition. The leakage current density versus electric field characteristics were investigated and compared with those of as-deposited and annealed pure $BiFeO_3$ (BFO) thin films. The dominant leakage mechanisms of nanocomposite films were space-charge-limited current and Poole–Frenkle emission for positive and negative biases, respectively. The leakage current density of nanocomposite films was reduced three orders of magnitude in comparison with the as-deposited pure BFO films. The less oxygen vacancies in the BFO phase in the nanocomposite is believed to contribute to the leakage reduction. © *2008 American Institute of Physics*.
[DOI: 10.1063/1.3000013]

Recently, multiferroic materials have attracted considerable interest for the simultaneous coexistence of ferroelectricity, (anti)ferromagnetism, and ferroelasticity.[1–6] $BiFeO_3$, which shows ferroelectricity with a Curie temperature (T_C) of ~1103 K and antiferromagnetic properties with a Néel temperature (T_N) of 643 K, is one of the most widely investigated multiferroic materials.[7] Epitaxial $BiFeO_3$ thin films with a remnant polarization of 55 $\mu C/cm^2$ have been fabricated by pulsed laser deposition (PLD).[1] This large polarization makes $BiFeO_3$ thin films very attractive for memory applications.[3] However, one of the main drawbacks that could limit the applications of this material is the high leakage current density, which is related to the oxygen vacancies and oxidation states of Fe.[8–11] Efforts have been made to reduce the leakage current density by either introducing dopants or using different fabrication methods.[9,10,12–17] We have recently demonstrated that the leakage current density can be greatly reduced by forming $(BiFeO_3)_{0.5}:(Sm_2O_3)_{0.5}$ nanocomposite films.[18] In the present work, we investigated the leakage mechanisms and the origin of the reduction of leakage current density in $(BiFeO_3)_{0.5}:(Sm_2O_3)_{0.5}$ nanocomposite films.

$(BiFeO_3)_{0.5}:(Sm_2O_3)_{0.5}$ nanocomposite films were deposited on (001) oriented conductive Nb-doped $SrTiO_3$ (Nb-STO) substrates by PLD. The experimental details have been described elsewhere.[19] The thickness of films, measured by transmission electron microscopy (TEM), is 150 nm. Analyses from both high-resolution x-ray diffraction and TEM revealed self-assembled epitaxial two-phase $BiFeO_3$ (BFO) and Sm_2O_3 (SmO) nanocomposites.[18,19] For comparison, pure BFO and SmO thin films with the same thickness were fabricated on (001) oriented Nb-STO substrates using the same processing parameters. To investigate the postannealing effect, some pure BFO thin films were subjected to an *in situ* annealing in oxygen (~500 Torr) at a temperature of 390 °C for 60 min. For electrical measurements, vertical sandwich capacitors with a configuration of Pt/BFO:SmO/Nb-STO (or Pt/BFO/Nb-STO and Pt/SmO/Nb-STO) were fabricated by depositing Pt top electrode with an area of 1×10^{-4} cm^2. The current-voltage characteristics were measured using a Keithley 487 picoammeter/voltage source with the delay time of 5 s. The polarity of bias is defined as negative or positive according to the negative or positive voltage applied to the Pt electrode. The film morphology was examined by scanning electron microscopy (SEM). To evaluate the optical refractive index, spectroscopic ellipsometry (SE) measurements (variable angle spectroscopic ellipsometor, J. A. Woollam Co., Inc.) were carried out at the incident angles of 60°, 65°, and 70°.

Figure 1 shows the leakage current density versus electric field (*J-E*) characteristics of as-deposited BFO, annealed BFO, nanocomposite BFO:SmO, and SmO thin films. The *J-E* characteristics of all the films at negative and positive

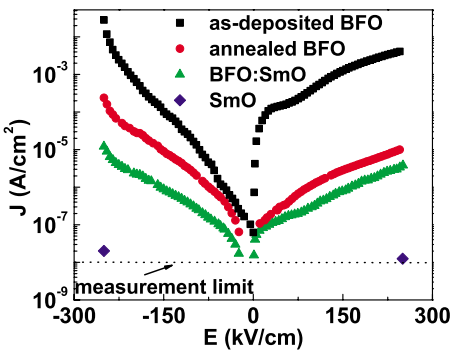

FIG. 1. (Color online) *J* vs *E* characteristics of as deposited BFO, annealed BFO, nanocomposite BFO:SmO, and SmO thin films. The dotted line shows the measurement limit.

a)Authors to whom correspondence should be addressed. Electronic addresses: hyang@lanl.gov and qxjia@lanl.gov.

biases are asymmetric; this may originate from the different work functions of Pt and Nb-STO electrodes.[20] It is clear that $J_{\text{as-depositedBFO}} \gg J_{\text{annealedBFO}} \gg J_{\text{BFO:SmO}} \gg J_{\text{SmO}}$ at a given electric field. Qi *et al.*[9] reported that oxygen vacancies rather than Fe^{2+} are the main cause for the high leakage current density in BFO. Many studies have shown that oxygen vacancies in ferroelectric thin film can be reduced by annealing the film in oxygen.[10,21] This may explain the lower leakage current density of the annealed BFO than that of the as-deposited BFO. It is worth noting that the leakage current density of BFO:SmO nanocomposite films is three orders of magnitude lower in comparison with as-deposited BFO films. Since the nanocomposite films were fabricated under the same conditions as those of as-deposited BFO films, there should be another reason rather than the annealing effect for the reduced leakage current density in the nanocomposite films.

To investigate the leakage behavior, we have considered three different leakage mechanisms: the Poole–Frenkel (PF) emission, the space-charge-limited current (SCLC), and the Fowler–Nordheim (FN) tunneling. If the leakage is controlled by the PF emission, which originates from the field-assisted thermal ionization of trapped carriers into the conduction band of thin films, the leakage current density can be expressed as[22,23]

$$J = AE \exp\left[\frac{-(\phi_t - e\sqrt{eE/\pi\varepsilon_{\text{opt}}\varepsilon_0})}{kT}\right], \tag{1}$$

where A is a constant, ϕ_t is the trap ionization energy, e is the elementary charge, T is the temperature, k is the Boltzmann's constant, ε_{opt} is the optical dielectric constant, and ε_0 is the permittivity of free space. On the other hand, if the leakage is dominated by the SCLC, which originates from the density of free electrons due to the carrier injection becoming greater than the density of thermally stimulated free electrons, the leakage current density can be expressed as[24]

$$J = \frac{9}{8}\varepsilon_r\varepsilon_0\mu\frac{E^2}{L}, \tag{2}$$

where μ is the mobility of charge carriers, ε_r is the relative dielectric constant, and L is the film thickness. Furthermore, if the leakage is controlled by the FN tunneling, the leakage current density can be expressed as[25]

$$J = BE^2 \exp\left(\frac{-C\phi_i^{3/2}}{E}\right), \tag{3}$$

where B and C are constants and ϕ_i is the potential barrier height. Therefore, the J-E characteristics of PF emission, FN tunneling, and SCLC can be characterized by the linear relationships of $\ln(J/E) - E^{1/2}$, $\ln(J/E^2) - (1/E)$, and $\log(J) - \log(E)$ with a slope around 2.

Figure 2 shows $\log(J)$ versus $\log(E)$ characteristics of as-deposited BFO, annealed BFO, and nanocomposite BFO:SmO films at positive bias. The slopes are close to 1 and the leakage currents show Ohmic behavior at relatively lower electric fields. In the high electric field range ($> \sim 75$ kV/cm), the $\log(J) - \log(E)$ plots are linear and the slopes are close to 2, which agree well with the SCLC mechanism. The SCLC is considered as a normal leakage behavior and correlates with oxygen vacancies in BFO materials.[9,10] In addition, we also studied the J-E characteristics of as-deposited BFO, annealed BFO, and BFO:SmO films at negative bias. In the low electric field range (<50 kV/cm), the $\log(J)$ versus $\log(E)$ plots are linear and the slopes are around 2 (not shown), indicating the conduction is controlled by SCLC. Figure 3 shows (a) $\ln(J/E^2)$ versus $(1/E)$ characteristic of as-deposited BFO film and (b) $\ln(J/E)$ versus $E^{1/2}$ characteristics of BFO:SmO and annealed BFO films at negative bias. For the as-deposited BFO film, the leakage currents show FN tunneling behavior in the electric field above 180 kV/cm. On the other hand, the $\ln(J/E) - E^{1/2}$ plots of BFO:SmO and annealed BFO films show linear relation in the electric field above 50 kV/cm. The ε_{opt} of BFO:SmO and annealed BFO films, with values of 6.45 and 5.19, respectively, can be calculated from the slopes of $\ln(J/E)$ versus $E^{1/2}$ plots.[26] The optical refractive index (n) can be determined from the optical dielectric constant with a relationship of $n = \sqrt{\varepsilon_{\text{opt}}}$. For BFO:SmO and annealed BFO films, the n can be evaluated as 2.54 and 2.28, respectively. The n can also be measured directly from the SE measurement through model based analysis. The measured n values are 2.42 and 2.58 at the wavelength of 633 nm for BFO:SmO and annealed BFO films, respectively. The n values calculated from slopes of $\ln(J/E)$ versus $E^{1/2}$ plots are in good agreement with the SE extracted results, strongly suggesting PF emission behavior in the electric field

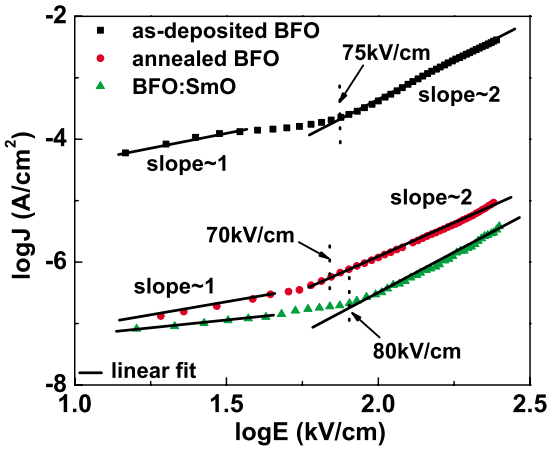

FIG. 2. (Color online) $\text{Log}(J)$ vs $\log(E)$ characteristics of as-deposited BFO, annealed BFO, and BFO:SmO thin films at positive bias.

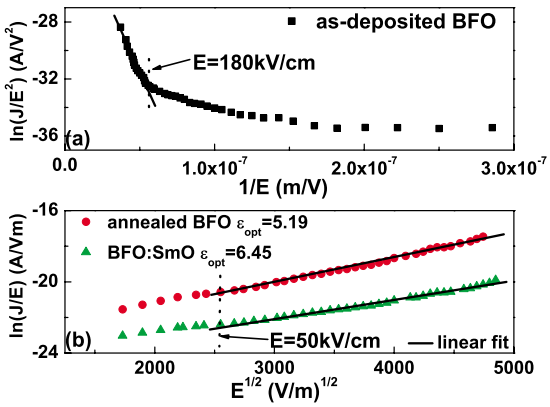

FIG. 3. (Color online) (a) $\text{Ln}(J/E^2)$ vs $(1/E)$ characteristic of as-deposited BFO film. (b) $\ln(J/E)$ vs $E^{1/2}$ characteristics of BFO:SmO and annealed BFO films at negative bias. The calculated optical dielectric constants are shown.

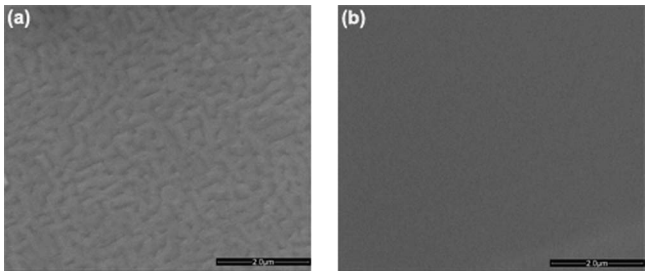

FIG. 4. SEM images of (a) as-deposited BFO film and (b) BFO:SmO nanocomposite.

range above 50 kV/cm. The PF emission is commonly considered as an acceptable leakage behavior and the likely trap center is Fe^{2+} in BFO films.[10,11] In summary, the leakage mechanisms of BFO:SmO nanocomposite films are the same as those of annealed BFO films.

As demonstrated by the cross-sectional TEM image, the BFO and SmO columns in nanocomposite films are connected in parallel with a device configuration of Pt/BFO:SmO/Nb-STO.[18] Because the leakage mechanisms of nanocomposite films are the same as those of the annealed BFO films and $\rho_{SmO} \gg \rho_{BFO:SmO} \gg \rho_{BFO}$ (ρ is the resistivity) in a given electric field, the leakage current in nanocomposite films should be controlled by the BFO phase. On the other hand, the reduction of oxygen vacancies, as we discussed earlier, can lead to the reduction of leakage current density in the annealed BFO films in comparison with the as-deposited BFO films. Therefore, the reduction of leakage current density in BFO:SmO nanocomposite films implies the reduced oxygen deficiencies in the BFO phase.

It should be noted that another possible origin of reduction of leakage current density is the change of film morphology. Normally, the grain boundaries are known to be high leakage current paths.[27] Then the increasing grain size should contribute to the reduction of leakage current.[28] Figure 4 shows the SEM images of (a) as-deposited BFO film and (b) BFO:SmO nanocomposite. Uniform grains with a size of 300 nm distributed homogeneously in the as-deposited BFO film. For BFO:SmO nanocomposite, no obvious feature was observed. This is mainly because of the small size of the BFO and SmO nanocolumn in the nanocomposite.[19] It is clear that the grain size of as-deposited BFO is much larger than that of BFO:SmO nanocomposite. Therefore, the morphology effect is not the origin of the reduction of leakage current density in the current study.

To illustrate the effects of the reduced leakage current density on the physical properties, we have compared the dielectric and ferroelectric properties of BFO:SmO nanocomposite with those of as-deposited BFO thin films. The dielectric loss of BFO:SmO nanocomposite is much lower than that of as-deposited BFO film.[18,19] This is consistent with reported results that ferroelectric material with lower leakage current typically shows smaller dielectric loss.[10] The polarization-electric field hysteresis loop of BFO:SmO nanocomposite was measured (not shown). Due to the low leakage current nature, a high electric field could be applied up to 2 MV/cm. A remnant polarization (P_r) of 23.3 $\mu C/cm^2$ was observed, remarkable higher than the value of as-deposited BFO film.

In conclusion, BFO:SmO nanocomposite films have been deposited on conductive Nb-STO substrates by PLD. The leakage mechanisms have been investigated and compared with those of as-deposited and annealed BFO films. For nanocomposite films, the dominant leakage mechanisms are SCLC and PF emission for positive and negative biases, respectively, which is the same as leakage mechanisms of annealed BFO films. The leakage current density of nanocomposite films is three orders of magnitude lower than that of as-deposited BFO films, which originates from the less oxygen deficiencies in the BFO phase. The present work represents an alternative approach to reduce leakage current density of BFO thin films by forming vertical nanocomposite architecture.

We gratefully acknowledge the support of the U.S. Department of Energy through the LANL/LDRD Program for this work.

[1] J. Wang, J. B. Neaton, H. Zheng, V. Nagarajan, S. B. Ogale, B. Liu, D. Viehland, V. Vaithyanathan, D. G. Schlom, U. V. Waghmare, N. A. Spaldin, K. M. Rabe, M. Wuttig, and R. Ramesh, Science **299**, 1719 (2003).
[2] F. Zavaliche, H. Zheng, L. Mohaddes-Ardabili, S. Y. Yang, Q. Zhan, P. Shafer, E. Reilly, R. Chopdekar, Y. Jia, P. Wright, D. G. Schlom, Y. Suzuki, and R. Ramesh, Nano Lett. **5**, 1793 (2005).
[3] H. Zheng, Q. Zhan, F. Zavaliche, M. Sherburne, F. Straub, M. P. Cruz, L. Q. Chen, U. Dahmen, and R. Ramesh, Nano Lett. **6**, 1401 (2006).
[4] S.-W. Cheong and M. Mostovoy, Nature Mater. **6**, 13 (2007).
[5] R. Ramesh and N. A. Spaldin, Nature Mater. **6**, 21 (2007).
[6] N. A. Spaldin and M. Fiebig, Science **309**, 391 (2005).
[7] C. Michel, J.-M. Moreau, G. D. Achenbach, R. Gerson, and W. J. James, Solid State Commun. **7**, 701 (1969).
[8] H. Yang, M. Jain, N. A. Suvorova, H. Zhou, H. M. Luo, D. M. Feldmann, P. C. Dowden, R. F. DePaula, S. R. Foltyn, and Q. X. Jia, Appl. Phys. Lett. **91**, 072911 (2007).
[9] X. Qi, J. Dho, R. Tomov, M. G. Blamire, and J. L. MacManus-Driscoll, Appl. Phys. Lett. **86**, 062903 (2005).
[10] C. Wang, M. Takahashi, H. Fujino, X. Zhao, E. Kume, T. Horiuchi, and S. Sakai, J. Appl. Phys. **99**, 054104 (2006).
[11] G. W. Pabst, L. W. Martin, Y. H. Chu, and R. Ramesh, Appl. Phys. Lett. **90**, 072902 (2007).
[12] S. K. Singh and H. Ishiwara, Jpn. J. Appl. Phys., Part 2 **44**, L734 (2005).
[13] G. L. Yuan and S. W. Or, Appl. Phys. Lett. **88**, 062905 (2006).
[14] J. K. Kim, S. S. Kim, and W. J. Kim, Appl. Phys. Lett. **88**, 132901 (2006).
[15] Y. Wang and C. W. Nan, Appl. Phys. Lett. **89**, 052903 (2006).
[16] S. R. Shannigrahi, A. Huang, N. Chandrasekhar, D. Tripathy, and A. O. Adeyeye, Appl. Phys. Lett. **90**, 022901 (2007).
[17] A. H. M. Gonzalez, A. Z. Simões, L. S. Cavalcante, E. Longo, J. A. Varela, and C. S. Riccardi, Appl. Phys. Lett. **90**, 052906 (2007).
[18] H. Yang, H. Wang, J. Yoon, M. Jain, D. M. Feldmann, P. C. Dowden, J. L. MacManus-Driscoll, and Q. X. Jia (unpublished).
[19] J. L. MacManus-Driscoll, P. Zerrer, H. Wang, H. Yang, J. Yoon, A. Fouchet, R. Yu, M. G. Blamire, and Q. X. Jia, Nature Mater. **7**, 314 (2008).
[20] S. J. Clark and J. Robertson, Appl. Phys. Lett. **90**, 132903 (2007).
[21] L. A. Knauss, J. M. Pond, J. S. Horwits, D. B. Chrisey, C. H. Mueller, and R. Treece, Appl. Phys. Lett. **69**, 25 (1996).
[22] P. Zubko, D. J. Jung, and J. F. Scott, J. Appl. Phys. **100**, 114113 (2006).
[23] Y. P. Wang and T. Y. Tseng, J. Appl. Phys. **81**, 6762 (1997).
[24] R. H. Tredgold, *Space Charge Conduction in Solids* (Elsevier Publishing Company, Amsterdam, 1965).
[25] S. M. Sze, *Physics of Semiconductor Devices*, 2nd ed. (Wiley, New York, 1981).
[26] From Eq. (1), a linear relationship between $\ln(J/E)$ and $E^{1/2}$ with a slope of $e\sqrt{e/\pi\varepsilon_{opt}\varepsilon_0}/kT$ should be obtained. The slope can be used to calculate the value of ε_{opt}.
[27] S. Saha and S. B. Krupnidhi, J. Appl. Phys. **88**, 3506 (2000).
[28] C. F. Chung and J. M. Wu, Electrochem. Solid-State Lett. **8**, F63 (2005).